Title

Genomic control of neuronal demographics in the retina

Authors

Reese, Benjamin E
Keeley, Patrick W

Publication Date

2016-11-01

DOI

10.1016/j.preteyeres.2016.07.003

Peer reviewed

HHS Public Access

Author manuscript

Prog Retin Eye Res. Author manuscript; available in PMC 2017 November 01.

Published in final edited form as:

Prog Retin Eye Res. 2016 November ; 55: 246–259. doi:10.1016/j.preteyeres.2016.07.003.

Genomic Control of Neuronal Demographics in the Retina

Benjamin E. Reese[1,2] and **Patrick W. Keeley**[1,3]

[1]Neuroscience Research Institute, University of California, Santa Barbara, CA 93106-5060 USA

[2]Department of Psychological & Brain Sciences, University of California, Santa Barbara, CA 93106-5060 USA

[3]Department of Molecular, Cellular & Developmental Biology, University of California, Santa Barbara, CA 93106-5060 USA

Abstract

The mature retinal architecture is composed of various types of neuron, each population differing in size and constrained to particular layers, wherein the cells achieve a characteristic patterning in their local organization. These demographic features of retinal nerve cell populations are each complex traits controlled by multiple genes affecting different processes during development, and their genetic determinants can be dissected by correlating variation in these traits with their genomic architecture across recombinant-inbred mouse strains. Using such a resource, we consider how the variation in the numbers of twelve different types of retinal neuron are independent of one another, including those sharing transcriptional regulation as well as those that are synaptically-connected, each mapping to distinct genomic loci. Using the populations of two retinal interneurons, the horizontal cells and the cholinergic amacrine cells, we present in further detail examples where the variation in neuronal number, as well as the variation in mosaic patterning or in laminar positioning, each maps to discrete genomic loci where allelic variants modulating these features must be present. At those loci, we identify candidate genes which, when rendered non-functional, alter those very demographic properties, and in turn, we identify candidate coding or regulatory variants that alter protein structure or gene expression, respectively, being prospective contributors to the variation in phenotype. This forward-genetic approach provides an alternative means for dissecting the molecular genetic control of neuronal population dynamics, with each genomic locus serving as a causal anchor from which we may ultimately understand the developmental principles responsible for the control of those traits.

Keywords

recombinant inbred strain; QTL; haplotype; SNP; gene variant; retinal mosaic

Address for correspondence: B.E. Reese, Neuroscience Research Institute, University of California, Santa Barbara, CA 93106-5060; breese@psych.ucsb.edu.

1. Introduction

The nervous system is assembled during development through various processes that control the size, the distribution, and the connectivity of different populations of neurons. Neuronal function, in turn, depends upon the effective outcome of these various developmental events, leading to the common presumption that there is an optimal number of neurons in each population in order to establish the proper ratio of afferent and target cells in a neuronal circuit. Indeed, different species exhibit conspicuous variation in both neuronal number and in the ratios of their pre-to post-synaptic populations, suggesting that such developmental processes are precisely controlled to ensure the neuronal wiring and connectivity that is unique to each species.

For instance, numerous studies have shown how manipulating the expression of a particular gene can yield conspicuous alterations in the proportions of different neuronal populations, for instance, increasing the numbers of some cell types at the expense of others. This approach has been most fruitfully employed in the study of fate assignment within the retina, where a hierarchical transcription factor code has been shown to modulate neuronal competence, determination and differentiation (Bassett and Wallace, 2012; Ohsawa and Kageyama, 2008; Xiang, 2013), and where the associated gene regulatory networks mediating these events are being dissected in increasing detail (Kwasnieski et al., 2012; Mu and Klein, 2008; Wang et al., 2014). Others studies have demonstrated how modifying the size of a target population of neurons during development can yield corresponding changes in the number of their afferents. Such target-dependency, best illustrated within the peripheral nervous system, has been shown to depend upon trophic factors that control cell survival (Cowan, 2001; Davies, 1996). “Quantitative (or numerical) matching” of pre- and post-synaptic populations was said to be achieved by such a mechanism, placing the critical control of neuronal number upon a target-dependent modulation of programmed cell death (Buss et al., 2006). Within the central nervous system, the retinal ganglion cell population has been one of the most thoroughly studied populations, having been shown to undergo substantial programmed cell death during development (Linden and Reese, 2006), where the amount of cell loss is modulated by the size of the target tissue (as well as by afferent innervation) and factors secreted therein (Spalding et al., 2004; Voyatzis et al., 2012). Together, these studies would suggest that the precision in neuronal number within the retina is regulated with exquisite cell-intrinsic transcriptional control but also modulated by target-dependent trophic support to establish the characteristic neuronal architecture and associated cellular ratios that underlie visual performance unique to each species (figure 1). We begin by considering the evidence for this presumption using the mouse retina.

2. Neuron number is precisely specified in the mouse retina

In order to examine the generality of these conclusions, we recently quantified the sizes of twelve different neuronal populations in the retina across a collection of 26 genetically distinct recombinant inbred mouse strains (Keeley et al., 2014a). Specifically, we sought to assess the extent to which the population size of retinal neurons is tightly controlled, and whether such specification serves to ensure consistent species-typical afferent-to-target cell ratios. These strains, the AXB/BXA strain-set, were originally derived from two parental

inbred laboratory strains (C57BL/6J, called B6/J hereafter, and A/J), each one of them being a unique mix, due to recombination during meiosis, of their respective haplotypes (abbreviated *B* versus *A*, respectively) throughout the genome (Williams et al., 2001) (figure 2). We sampled the populations of rod and cone photoreceptors, horizontal cells, four types of bipolar cells, and five different populations of amacrine cells (figure 3A), populations that can be reliably determined and discriminated from other cells of the same class. These different populations exhibit a massive range in their absolute numbers, from millions of rod photoreceptors to as few as hundreds of dopaminergic amacrine cells (figure 3B). Despite this enormous variation in number between the cell types, we found the range of variation for any particular cell type in a strain to be limited, and fairly consistent, across the twelve cell types. For example, the coefficient of variation (CoV), averaged across the 26 strains, ranged from a low of 0.030 for the VGluT3+ amacrine cell population, to a high of 0.065 for the Type 4 cone bipolar cell population (figure 3C).

We expected to find that estimating the size of larger populations through sampling only a small proportion of total retinal area would lead to greater variability across individuals, yet we found no such correlation between population size and CoV: for instance, we found a comparably low average CoV for the largest neuronal population (the rod photoreceptors, being 0.036), for which we had sampled only ~0.1% of total retinal area, as we did for the sparsest neuronal population (the dopaminergic amacrine cells, having an average CoV of 0.045), for which we sampled the entirety of the retina (Keeley et al., 2014a). As every individual mouse within each strain should be genetically identical, this variation observed within any strain should arise from some combination of technical or sampling variance plus that due to any intrinsic variability in biological processes governing the determination of cell number (see Keeley et al., 2016, for a fuller consideration of this point). That these non-genetic contributions yielded relatively meager variation would indicate an impressive degree of precision in the control of neuronal number. Indeed, one may marvel as much at the fidelity by which the developing retina produces a precise if tiny number of cells (the dopaminergic amacrine cells, totaling ~0.01% of all retinal neurons) as when it consistently produces a precise if enormous number (the rod photoreceptors, totaling about three-quarters of all retinal neurons; (Jeon et al., 1998; Macosko et al., 2015).

3. Different strains of mice show considerable variation in neuron number

This degree of control over neuronal number within a strain is the more remarkable when considering the terrific variation in number *between* the strains, for every cell type. For instance, the population of rod photoreceptors increases, from the strain with the lowest number (having 6,051,100 cells) to the strain with the highest number (with 8,227,260 cells), by 36%. The population of Type 3b cone bipolar cells shows a 60% increase, and that for the horizontal cells shows a 92% increase, while the population of dopaminergic amacrine cells increases by 298% (Keeley et al., 2014a) (figure 3C). For every one of these different cell types, the variation in cell number (from the strain with the lowest number to the strain with the highest number) is graded, rather than conspicuously step-like with discrete phenotypic groupings of the strains (histograms in figure 3B), indicating that cell number must be a complex trait controlled by multiple genes for which variants discriminate the two parental genomes. Nerve cell number, therefore, varies substantially across these different mouse

strains, due to the actions of allelic variants in many genes. Imagine how many more variants would be brought into play on a mixed genetic background like our own.

4. Variation in neuron number is largely uncorrelated between different cell types

We can use this dataset on neuronal number, derived from twelve different cell types across 26 genetically distinct recombinant inbred strains, to determine the extent to which different pairs of cell types have their numbers correlated, either positively or negatively. Figure 4A displays this correlation matrix for every pair-wise comparison within the dataset, indicating the Pearson correlation coefficient (r) for each linear regression. It shows that, for most pairs of cell types, no significant correlation between them exists. Considering first the populations of cells that are synaptically connected to one another, which define the radial transmission of visual information through the retina, there is no significant correlation between the number of cones with any of the three types of cone bipolar cell (e.g. figure 4B), between the number of rods with the rod bipolar cells, nor between the number of rod bipolar cells with their postsynaptic target, the AII amacrine cells. Considering those cell types of the same major classes, there is not a hint of a negative correlation between any pairs of cell types, and rarely a significant positive correlation. For instance, the numbers of rod and cone photoreceptors are not significantly correlated (figure 4C), though their numbers have been shown to be inversely regulated by transcription factors governing cell fate specification and terminal differentiation (Swaroop et al., 2010). Neither are the numbers of the three cone bipolar cell types significantly correlated, though their numbers might have been expected to be positively correlated in the process of stipulating the overall size of the OFF cone bipolar cell population, or to be negatively correlated as OFF cone bipolar cells differentiate into one, rather than another, OFF cone bipolar type. Likewise, most types of amacrine cell show no significant correlation with other amacrine cell types, although there is one notable exception, being the correlation between the number of cholinergic amacrine cells in the INL versus the number in the GCL (figure 4D). This strong positive correlation would be the exception that proves the rule: our lack of detecting strong correlations between any of the other cell types is not some consequence of working with a strain-set comprised of only 26 strains. These results point to a strong degree of developmental relatedness between the two types of cholinergic amacrine cell (Whitney et al., 2014), as might have been expected given their similar morphologies and functional contributions to ON versus OFF processing of directional movement (Vaney et al., 2012). What is unexpected is the absence of any strong positive or negative correlations between the various other cell types.

5. Genetic manipulations altering the number of afferents or targets do not modulate the size of neuronal populations in the mouse retina

The results in figure 4 would suggest that the final number of a given type of neuron in the retina is largely independent of the number of other cells that share transcriptional regulatory control during development. They also suggest that neuronal number is largely independent of the number of other cells that are synaptically connected to that population. This latter

conclusion is bolstered by a variety of other manipulation studies within the retina showing that altering the number of target cells, like altering the number of afferents, does not change the size of a synaptically-connected population of neurons therein (e.g. Strettoi and Volpini, 2002). For instance, the early elimination of the population of cone photoreceptors, in the coneless mutant mouse (figure 5A), affects neither the number of target horizontal cells, which are generated contemporaneously with the cones (Raven and Reese, 2003), nor the numbers of three different types of OFF cone bipolar cells (Keeley et al., 2014c), which are all generated after the cone photoreceptors (Young, 1985). Likewise, the ultimate size of the cone photoreceptor population is not altered by doubling or halving the thickness of the inner nuclear layer during early development, within which the numbers of multiple types of ON and OFF cone bipolar cells are modulated up or down (Lee et al., 2011) (figure 5B), nor by reducing the number of horizontal cells extending dendrites into the outer plexiform layer (Keeley et al., 2013) (figure 5C). And doubling the number of retinal ganglion cells does not alter the size of three different OFF cone bipolar cell populations (Keeley et al., 2014c) (figure 5D). The numbers of these OFF cone bipolar cell types have each been shown to be modulated via *Bax*-mediated cell death during development, so it is particularly surprising that altering neither their cone afferents (figure 5A) nor their ganglion cell targets (figure 5D) modulates the degree of this loss (Keeley et al., 2014c).

6. Variation in neuron number maps to independent genomic loci for each cell type

The above results demonstrate that neuronal number, at least within the retina, has little dependency on the size of other transcriptionally-related or synaptically-connected neuronal populations. The former conclusion is not to dismiss the role of such transcriptional control during retinal development; only that variants in those genes are unlikely to contribute substantially to the variation observed across these strains. Rather, these results show that there must be multiple other factors normally controlling the final number of neurons in the retina, and would suggest that these factors disproportionately alter neuronal number across different types of retinal neurons. This is borne out when considering how the variation in neuron number, across the strains, maps to distinct genomic loci for each cell type. Because each of these strains has been genotyped at high density for single nucleotide polymorphisms (SNPs) and microsatellite markers (Williams et al., 2001), we can assess the degree of linkage between genotype with phenotype by comparing the variation in *A* versus *B* haplotype across the strains with the variation in their number of cells (figure 2). Such “quantitative trait locus” (QTL) mapping reveals unique genomic loci for every cell type (figure 6). Each of these genomic maps shows the strength of this linkage across the genome (the likelihood ratio statistic, or LRS score), drawing our attention to those most prominent loci containing genetic variants that modulate retinal cell number. The fact that they do not all coincide at the same genomic locus shows that there is no single determinant responsible for the variation in population sizes, for instance, that such variation cannot be a simple consequence of a genetic variant controlling proliferation, yielding differences in the overall size of the retina. The strongest loci identified for each cell type (with the exception of the cholinergic amacrine cells in the GCL) is associated with a sizable proportion of the range

exhibited for each of the cell types indicated in figure 3C, accounting for 23–40% of that range (Keeley et al., 2014a).

7. Multiple variant genes contribute to the variation in cell number

While some of the genomic maps reveal only a single conspicuous peak, there may be multiple genetic variants residing within that locus exerting distinctive and independent contributions in setting retinal cell number. For instance, the variation in dopaminergic amacrine cell number maps a broad genomic locus on Chr 7 (figure 6), where at least three independent genes have been shown to contribute to the variation in dopaminergic amacrine cell number observed across these recombinant inbred strains (Whitney et al., 2009). Other genomic maps in figure 6 contain multiple QTLs on different chromosomes, for instance, that for the variation in Type 3b cone bipolar cell number. Here, the two largest QTL are located on Chrs 3 and 6, and the effects attributed to each locus have countervailing influences: the strains containing the *B* haplotype at the Chr 3 locus have higher Type 3b cone bipolar cell numbers, while the strains containing the *B* haplotype at the Chr 6 locus have lower numbers (Keeley et al., submitted). This should contribute to the fact that the parental strains barely differ in their number of this type of cone bipolar cell, despite the large variation across the set of recombinant inbred strains (shown in figure 3B): some of the strains will have the *A* haplotype at one locus and the *B* haplotype at the other (as well as at other controlling loci), and so will contain numbers of bipolar cells that may be higher or lower than either of the two parental strains (Keeley et al., 2014a).

8. Identifying candidate genes modulating neuron number

The genetic variants operating at each of these loci may be exerting their effects by modulating distinct biological processes, for instance, by affecting programmed cell death or by altering cell fate assignment. They may be regulatory variants, affecting transcript levels, or they may be coding variants, altering or disrupting a functional protein. Various strategies can be pursued to assess a gene from amongst the collection of candidates at a given locus. One approach is to examine its loss of function upon retinal development, thereby confirming that the gene does indeed modulate the number of the very cell type in question. Consider, for example, the QTL for horizontal cell number on Chr 13 (figure 7B), where the *B* haplotype is associated with a sizeable increase in the number of horizontal cells (a QTL effect amounting to 28% of the range in variation across the strain-set) (figure 7A). Positioned at this locus is the LIM homeodomain transcription factor gene, *Isl1* (figure 7B), and the conditional knock-out of *Isl1* during ocular development yields a 41% increase in the density of horizontal cells in the central retina relative to littermate control mice (Whitney et al., 2011b) (figure 7C). Sequence analysis reveals only synonymous (non-functional) coding variants discriminating the two parental genomes, but multiple SNPs are also present in potential regulatory regions of the *Isl1* gene (figure 7D). That differences in *Isl1* expression might relate to the variation in horizontal cell number is supported by the negative correlation between horizontal cell number and *Isl1* expression (figure 7E), assessed using microarray analysis of ocular mRNA for each strain (Whitney et al., 2011a). Quantitative PCR confirmed differences in *Isl1* expression in maturity (> twofold), as well as during the period of horizontal cell genesis, on embryonic day 13.5 (> four-fold), with the

A/J strain showing higher levels of expression (figure 7F). That such differences in *Isl1* expression reflect the action of a *cis*-modulatory variant was further supported by an allele-specific expression assay, revealing a greater number of *A* relative to *B Isl1* transcripts in the F1 progeny generated from a parental cross that could not be ascribed to any difference in amplification efficiency discriminating the genomic sequence (figure 7G) (Whitney et al., 2011b). Given such differences in expression, one can, in turn, interrogate those prospective regulatory SNPs to identify any predicted to create/disrupt novel transcription factor binding sites. Indeed, one such variant in a hexanucleotide sequence in the 5′ UTR establishes an E-box due to the *B* variant (figure 7D, inset), being a binding site for bHLH transcription factors, some of which are known to repress transcription (Fischer and Gessler, 2007). Curiously, it is the *A* variant that is the conserved sequence across mammals. Binding at this E-box may therefore disrupt some other conserved motif that normally serves to drive *Isl1* expression, lowering transcript levels in strains carrying the *B* variant (e.g. Thiel et al., 2004).

Together, these studies in figure 7 support the view that a regulatory variant, possibly this particular SNP, discriminating the two parental genomes modulates *Isl1* expression, in turn contributing to the variation in horizontal cell number. Such a forward-genetic approach, beginning with an analysis of cell number across the collection of recombinant inbred strains, can thereby facilitate the identification of genes controlling the size of a neuronal population, which can be further pursued to define their role in the developmental processes that modulate, for instance, neuronal production or survival. Furthermore, this strategy can be applied to any quantifiable trait, including other demographic features that characterize neuronal populations in the retina.

9. Gene variants modulate the local patterning of retinal mosaics

These populations of retinal neurons are organized as “mosaics” (Wässle & Riemann, 1978), where the patterning in their local spatial distribution is typically, although not always, found to be more orderly than for a random distribution of similarly sized cells at the same density (Reese, 2008a). Different types of retinal neuron vary in the degree of orderliness (or “regularity”) attained by their mosaics, but in general, the key to understanding how such patterning is generated lies in the local interactions between neighboring cells. Assessing the local “spacing rules”, either as a function of development, or in genetically modified retinas (Kay et al., 2012; Raven et al., 2005b), and defining the relationship between such variation in spacing with the variation in mosaic regularity, has shed light on the biological events underlying such patterned distributions of nerve cells (Reese and Keeley, 2015).

While one might expect that variation in the number of a particular type of retinal neuron should be a major contributor to intercellular spacing, and in turn, to mosaic regularity, multiple studies have revealed that the variation in local spacing (specifically, the effective radius; Cook, 1996) which correlates with the variation in cell density, shows little or no correlation with the variation in mosaic order. Where there is a slight negative correlation between the variation in density with regularity (Whitney et al., 2008), such variation in regularity has been shown to map, across this same recombinant inbred strain-set, to genomic loci distinct from those QTL mapped for the variation in cell number or cell

density. For instance, the population of retinal horizontal cells shows a nearly two-fold variation in cell number (figure 3b), and this variation maps to a genomic locus on Chr 13 mentioned above (figure 6) (Whitney et al., 2011b), yet the variation in the regularity of the horizontal cell mosaic across the strains maps to distinctive genomic loci on Chrs 1 and 14 (Keeley and Reese, 2014). Cholinergic amacrine cells also show a conspicuous if less pronounced variation in their number across the same strain-set, being a roughly 50% increase from the lowest to the highest strain (figure 3C), and this maps to two suggestive QTLs on Chrs 13 and 16 (figure 6), for the population in the inner nuclear layer. The variation in the regularity of this population, by contrast, maps to a different locus, on Chr 11 (figure 8B). At this locus, the *B* haplotype is associated with an increase in regularity across the strains (figure 8A), and this was confirmed by examining the consomic (chromosome substitution) strain B6.A<11>, which possesses the *A* haplotype for Chr 11 introgressed upon the B6/J genetic background (Singer et al., 2004). These mice show a decrease in mosaic regularity of a magnitude predicted by the size of the QTL effect, with many more pairs of cells being positioned side-by-side (Keeley et al., 2014b) (figure 8C).

Of the genes present at this locus on Chr 11, pituitary tumor transforming gene 1 (*Pttg1*) stood out as a strong candidate (figure 8B), for multiple reasons. First, its own expression across these recombinant inbred strains showed a positive correlation with regularity ($r = 0.47$) (figure 8D). This variation in *Pttg1* expression across the strain-set also mapped to the same genomic locus (an eQTL), suggesting the presence of a *cis*-regulatory variant controlling expression (figure 8E). Second, the B6/J and A/J strains are discriminated by a seven nucleotide INDEL at the transcriptional start-site (the only sequence variant associated with *Pttg1*), providing a candidate variant in the promoter that may be responsible for this difference in expression (figure 8F). Indeed, qPCR confirmed significantly greater expression of *Pttg1* in mature C57BL/6J retina relative to A/J retina, while an *in vitro* luciferase assay, in turn, confirmed the *A* variant to be significantly less effective in driving expression relative to the *B* variant (figure 8G). Finally, *Pttg1* was shown to modulate the mosaic regularity of this same population of retinal neurons, as its knockout showed a reduction in mosaic order coupled to an increase in the frequency of neighboring cells that failed to space themselves apart (Keeley et al., 2014b) (figure 8H).

Pttg1 is likely to exert its effects upon local cell-cell interactions as a transcriptional regulator (Tong and Eigler, 2009), and while its ultimate mechanism of action upon intercellular spacing remains to be determined, this and other studies reveal that the genetic underpinnings of mosaic patterning are distinct from those driving cell number (Kay et al., 2012). While variants modulating fate assignment or cell survival might have been expected to impact cellular patterning as well as final cell number, the lack of coincidence between their respective controlling genomic loci suggests quite distinctive processes involving genes modulating cell-cell interactions after final cell number is established.

10. Gene variants modulate cellular positioning within the retinal architecture

The correlation between the sizes of the populations of cholinergic amacrine cells in the INL and the GCL (figure 4D) suggested a unique degree of relatedness between them, consistent with the view that they arise from a single population that is subsequently divided into two independent sub-populations (Kim et al., 2000), each forming its own respective retinal mosaic on opposing sides of the emerging inner synaptic layer (figure 1). The population in the ganglion cell layer in maturity is conspicuously less orderly than the population in the inner nuclear layer, though this appears to be largely a consequence of the passive lateral displacement of neurons in the ganglion cell layer as the vasculature and optic fiber bundles form and settle amongst the neurons in this layer (Whitney et al., 2008). While the sizes of these two populations of cholinergic amacrine cells are highly correlated to one another (figure 4D), they are not perfectly matched in number, always being more numerous in the INL in the mouse retina (Whitney et al., 2014). In each of the two parental strains, B6/J and A/J, the ratio of cells in the two layers (GCL/INL) was identical, being 0.86 for each strain, falling close to the overall average across the recombinant inbred strain-set. Yet across those 26 strains, this ratio varied, from a low of 0.75 to a high of 0.95 (figure 9A) (being the residual variance shown in figure 4D), and was largely independent of the variation in total cholinergic amacrine cell number (figure 9C), indicating a heritable contribution in the allocation of a cholinergic amacrine cell to one or the other population. Indeed, the variation in this ratio trait mapped to a unique location in the genome, on Chr 3 (figure 9B), where a gene or genes containing variants between the two parental strains must modulate one or another biological process that alters their positioning between the two layers (Whitney et al., 2014).

One particular candidate at this locus stood out, being *Sox2* (figure 9B). *Sox2* is one of four stem cell transcription factor genes that are sufficient for maintaining pluripotency and for reprogramming differentiated cells (Pei, 2009). *Sox2* is expressed in all retinal progenitors (Ferri et al., 2004), and is critical for maintaining this progenitor pool for normal ocular development (Matsushima et al., 2011; Taranova et al., 2006), as *Sox2* mutations in humans cause anophthalmia or microphthalmia (Fantes et al., 2003; Schneider et al., 2009), a condition mimicked by a hypomorphic allele in mice (Taranova et al., 2006). *Sox2* also contains a functional variant discriminating the two parental strains, being a six nucleotide INDEL that extends a polyglycine tract due to the *B* variant (figure 9D). Curiously, *Sox2* continues to be expressed into maturity in only one type of retinal neuron, the cholinergic amacrine cell (figure 9E), and is the most highly expressed gene in cholinergic amacrine cells during postnatal development found at this genomic locus (Whitney et al., 2014). The maintained expression of *Sox2* in cholinergic neurons would suggest some novel function uniquely associated with their development.

To test this, conditional knockout mice were generated to remove *Sox2* exclusively from the cholinergic amacrine cells as they initiate their differentiation as cholinergic neurons (Whitney et al., 2014). Their retinas achieve normal size and architecture, and the total number of cholinergic amacrine cells in these retinas is not significantly different from

littermate control retinas, but their distribution between the two layers is conspicuously altered, there now being nearly twice as many cholinergic amacrine cells in the INL relative to the GCL (figure 9F). While this rearrangement might suggest that the role of Sox2 is associated with proper migration of cells that are normally destined for the ganglion cell layer, the cholinergic amacrine cells in both layers of such *Sox2*-conditional knockout retinas exhibit other morphological and molecular changes as well, suggesting instead some alteration in the assignment of sub-type identity amongst all cholinergic amacrine cells (Whitney et al., 2014). For instance, the P2×2 receptor, normally present on cholinergic amacrine cells in the inner nuclear layer, is abolished in the Sox2-conditional knockout retina, while many of the cholinergic amacrine cells in the ganglion cell layer differentiate bistratified dendritic arbors, extending processes that arborize in both cholinergic strata in the inner synaptic layer (figure 9G). The presence of bistratified dendrites is not observed in either the B6/J and A/J parental strains, however, so exactly how the INDEL might differentially modulate the role of Sox2 in controlling cellular positioning, while not affecting these other functions of Sox2, is not immediately clear. As the polyglycine tract resides outside of the DNA binding domain, perhaps it serves to modulate DNA-binding stability in association with a co-factor expressed by cholinergic amacrine cells. The fact that the polyglycine tract is conserved across other mammalian orthologs of the SoxB1 family members (Katoh and Katoh, 2005; Mojsin et al., 2010), and that such polyglycine tracts are frequently found in transcription factors (Albà and Guigó, 2004), would together support the hypothesis that this *Sox2* variant should be functional, contributing to the variation in cholinergic positioning that maps to this genomic locus.

11. Functional consequences of the independent control of neuronal number

The retina of each of these different mouse strains has its own unique proportions of these twelve different cell types (figure 10). In all likelihood, this variability in the size of these neuronal populations extends to all 85 or so of the different cell types present in the mouse retina (Sanes and Masland, 2015), but to date the only other support for this assumption stems from an analysis of the size of the total retinal ganglion cell population, showing conspicuous variation between different inbred laboratory strains (Williams et al., 1996). There is no reason to assume we had fortuitously sampled from only those cellular populations showing such variability, nor that the AXB/BXA strain-set encapsulates the maximum range of variation present in the mouse retina; those other inbred laboratory strains may exhibit even greater differences in the sizes of some of these neuronal populations, as has been demonstrated for the dopaminergic amacrine cells (Whitney et al., 2009). Indeed, given the right mix of genetic variants, a mouse retina might contain ratios between certain cell types approaching those characteristic of other species. For instance, the BXA12 recombinant inbred strain contains two cones for every one Type 3b OFF cone bipolar cell; one can envision the additive effects of other variants yielding even a one-to-one ratio in the mouse retina, being the cone-to-midget bipolar cell ratio in the primate's fovea (albeit lacking the dense packing therein).

The majority of the genetic variants frequenting the landscape of the mouse genome are believed to derive from differences that arose amongst isolated founder populations in the wild, well before the modern era of mouse breeding, being the source of much phenotypic variation present between different inbred laboratory mice (Reuveni et al., 2010). Genetically diverse populations such as ours may likewise harbor a degree of independent variability in the sizes (and therefore ratios) of their various retinal cell populations, though this has been supported by only a couple of studies in primates, examining the density of cone photoreceptors at the human fovea, which shows a 1.8-fold variation between individuals (Zhang et al., 2015), or the total number of retinal ganglion cells in the rhesus monkey, varying from 1.4 to 1.8 million cells (Spear et al., 1996). Whether differences in visual function accrue as a consequence has yet to be determined, but an increase in foveal cone density might not necessarily translate into increased acuity without a corresponding increase in midget bipolar and ganglion cell densities at the fovea (Rossi and Roorda, 2010). The optical resolution of the mouse eye, as well as the Nyquist limit for each population of (cone as well as rod) photoreceptors, far surpasses the behavioral resolution of the mouse, suggesting a post-receptoral constraint upon resolution perhaps associated with a particular type of ganglion cell critical for mediating behavioral acuity (Geng et al., 2011). In principle, variation in the size of this population should yield a corresponding change in visual resolution, assuming dendritic field area scales inversely with cell density. Indeed, in the primate retina, midget retinal ganglion cells extend their dendritic arbors to tile the retina in a density-dependent fashion (Dacey, 1993), setting the grain for visual acuity across the retinal surface (Rossi and Roorda, 2010).

While this assumption of dendritic tiling appears to be valid for most populations of retinal bipolar cells in the mouse retina (Lee et al., 2011; Wässle et al., 2009; but see Helmstaedter et al., 2013), it has not yet been demonstrated for any single population of mouse retinal ganglion cells; to the contrary, some ganglion cell classes in the mouse do not tile the retina, extending their dendrites to overlap with neighboring cells of the same type (Bleckert et al., 2014; Huberman et al., 2009; Kay et al., 2011; Rivlin-Etzion et al., 2011). Recent physiological evidence would suggest that this may be the norm for nearly all of the ~30 different types of ganglion cell in the mouse retina (Baden et al., 2016). Such overlap is characteristic of many other types of retinal neuron, wherein some types engage in homotypic regulation of their dendritic growth while others do not modulate that growth in association with any variation in local density (Reese and Keeley, 2015). For example, the horizontal cells, a cell type that undergoes a nearly two-fold variation in number across mouse strains, modulate their dendritic field areas inversely with density (up to a limit) to maintain a uniform dendritic coverage factor around six (Keeley et al., 2013; Poché et al., 2008; Reese et al., 2005). As these cells are interconnected via gap junctions under ambient illumination that may be typical for the mouse, their functional properties may not be substantially impacted by such variation in number (Dorgau et al., 2015; Xin and Bloomfield, 1999), though any variation in such gap junctional connectivity has yet to be assessed. Cholinergic amacrine cells, by contrast, exhibit some 30-fold dendritic overlap with neighboring like-type cells, yet this cell type does not show an inverse relationship between dendritic field area and cell density between strains that differ in their number (Keeley et al., 2007), and nor do these cells expand their dendritic fields following early

depletion of their like-type neighbors (Farajian et al., 2004). Variation in the number of this cell type, therefore, would impact retinal coverage, and may in turn affect the efficiency by which directional selectivity is computed for direction-selective retinal ganglion cell types (Vaney et al., 2012).

Two other retinal cell types that do not modulate their dendritic growth proportionately with their variation in density are the dopaminergic amacrine cells and the melanopsin-positive M1 retinal ganglion cells. The dopaminergic amacrine cells show the greatest variation in cell number across these strains, yet they do not reduce the size of their dendritic arbors accordingly when cell number is increased by a factor of four (Keeley and Reese, 2010a). Whether this cell type modulates the release of dopamine inversely with variation in the density of dopaminergic processes remains to be seen. The M1 (melanopsin-positive) retinal ganglion cells do not modulate the size of their dendritic fields when the frequency of like-type neighbors is reduced (Lin et al., 2004), but there may be little functional need to do so as irradiance detectors. Yet recent studies have shown these cells to also receive input from rods and cones, and that this input to the M1 ganglion cells is critical for rod/cone-driven photoentrainment of circadian rhythms, so any variation in the density and spacing of these cells between different mouse strains (yet to be assessed) might be predicted to affect circadian entrainment (Chen et al., 2013).

Consider as well the conspicuous variation in cone photoreceptor number across the AXB/BXA strain-set, varying from 116,000 to 204,000 cones. While this variation would be expected to affect photopic threshold, it should also be noted that there is no direct correlation between cone opsin gene expression and cone photoreceptor number across the recombinant inbred strain-set. Other variants are acting independently to modulate transcription across the strains, and one can envision yet others that might alter features affecting sensitivity, for instance, outer segment length, etc.

For those cell types that modulate dendritic growth inversely with cell density, this may suggest a means of conserving a constant level of dendritic coverage that may be more critical for retinal function than absolute cell density (Reese et al., 2011), at least for retinal neurons upstream of the ganglion cells (but see Freeman et al., 2015). One might similarly question the functional significance of any variation in the mosaic orderliness of a neuronal population if their dendritic arbors engage in homotypic interactions to regulate the overall size of the field in order to maintain a constant dendritic coverage, as is the case for the populations of bipolar cells and the horizontal cells (Reese et al., 2011). For example, the somata of Type 2 OFF cone bipolar cells are distributed in their array no different from the patterning achieved by a random distribution of similarly sized cells (Keeley et al., 2014b). Where dendritic arbors do *not* interact homotypically though (e.g. the cholinergic amacrine cells), spacing cells apart in a manner that gives rise to regularity in a retinal mosaic should be functionally beneficial, ensuring that the integrated profiles of the receptive fields of such a population of cells will be more uniform than that for a population that is randomly distributed. Testing directly, however, for any functional consequence of the variation in mosaic regularity (like that for the variation in number of a particular type of retinal cell) across the recombinant inbred strain-set, would be difficult, given all of the other variables present in each of the retinas of these different strains (e.g. figure 10). Functional

assessments across the strain-set, would, however, provide a trait that itself can be mapped and correlated with these other gene expression and anatomical traits that in turn may suggest avenues for further exploration.

The benefits of engaging in the pursuit of the genetic determinants of these population dynamics is that one may gain insight into their development, specifically, into the genetic and molecular control of the processes commanding their establishment. These may, in turn, lead to more selective genetically modified mouse models wherein one may come closer to isolating a single variable in order to examine the physiological or behavioral consequences of such selectively altered demographics. One must, of course, remain alert to the possibility that still other unexpected compensatory changes partially mitigate, or obscure the interpretation of, any functional deficits (Hassan and Hiesinger, 2015). Much as a dendritic arbor can be modulated by proximity to like-type neighbors, for some cell types, so we might also expect other forms of regulation, in some cases even ensuring the functional fidelity of a neuronal population despite variation in its size, patterning or positioning. By proceeding cautiously, we may ultimately come to understand how variation in such demographic traits is not only established during development but also how it affects visual performance.

Acknowledgments

Supported by NIH grants EY-11087 and EY-19968

References

Albà MM, Guigó R. Comparative analysis of amino acid repeats in rodents and humans. Genome Res. 2004; 14:549–554. [PubMed: 15059995]

Baden T, et al. The functional diversity of retinal ganglion cells in the mouse. Nature. 2016; 529:345–350. [PubMed: 26735013]

Bassett EA, Wallace VA. Cell fate determination in the vertebrate retina. Trends Neurosci. 2012; 35:565–573. [PubMed: 22704732]

Bleckert A, et al. Visual space is represented by nonmatching topographies of distinct mouse retinal ganglion cell types. Curr. Biol. 2014; 24:310–315. [PubMed: 24440397]

Buss RR, Sun W, Oppenheim RW. Adaptive roles of programmed cell death during nervous system development. Ann. Rev. Neurosci. 2006; 29:1–35. [PubMed: 16776578]

Chen S-K, et al. Apoptosis regulates ipRGC spacing necessary for rods and cones to drive circadian photoentrainment. Neuron. 2013; 77:503–515. [PubMed: 23395376]

Cook JE. Spatial properties of retinal mosaics: An empirical evaluation of some existing measures. Vis. Neurosci. 1996; 13:15–30. [PubMed: 8730986]

Cowan WM. Viktor Hamburger and Rita Levi-Montalcini: the path to the discovery of nerve growth factor. Ann. Rev. Neurosci. 2001; 24:551–600. [PubMed: 11283321]

Dacey DM. The mosaic of midget ganglion cells in the human retina. J. Neurosci. 1993; 13:5334–5355. [PubMed: 8254378]

Davies AM. The neurotrophic hypothesis: where does it stand? Phil. Trans. R. Soc. Lond. B. 1996; 351:389–394. [PubMed: 8730776]

Dorgau B, et al. Connexin50 couples axon terminals of mouse horizontal cells by homotypic gap junctions. J. Comp. Neurol. 2015 in press.

Fantes J, et al. Mutations in SOX2 cause anophthalmia. Nat. Genet. 2003; 33:461–463. [PubMed: 12612584]

Farajian R, et al. Cellular positioning and dendritic field size of cholinergic amacrine cells are impervious to early ablation of neighboring cells in the mouse retina. Vis. Neurosci. 2004; 21:13–22. [PubMed: 15137578]

Ferri AL, et al. Sox2 deficiency causes neurodegeneration and impaired neurogenesis in the adult mouse brain. Development. 2004; 131:3805–3819. [PubMed: 15240551]

Fischer A, Gessler M. Delta-Notch—and then? Protein interactions and proposed modes of repression by Hes and Hey bHLH factors. Nucleic Acids Res. 2007; 35:4583–4596. [PubMed: 17586813]

Freeman J, et al. Mapping nonlinear receptive field structure in primate retina at single cone resolution. eLife. 2015; 4:e05241. [PubMed: 26517879]

Geng Y, et al. Optical properties of the mouse eye. Biomed. Opt. Express. 2011:717–738. [PubMed: 21483598]

Hassan BA, Hiesinger PR. Beyond molecular codes: Simple rules to wire complex brains. Cell. 2015; 163:285–291. [PubMed: 26451480]

Helmstaedter M, et al. Connectomic reconstruction of the inner plexiform layer in the mouse retina. Nature. 2013; 500:168–174. [PubMed: 23925239]

Huberman AD, et al. Genetic identification of an On-Off direction-selective retinal ganglion cell subtype reveals a layer-specific subcortical map of posterior motion. Neuron. 2009; 62:327–334. [PubMed: 19447089]

Jeon C-J, Strettoi E, Masland RH. The major cell populations of the mouse retina. J. Neurosci. 1998; 18:8936–8946. [PubMed: 9786999]

Katoh Y, Katoh M. Comparative genomics on SOX2 orthologs. Oncol. Rep. 2005; 14:797–800. [PubMed: 16077994]

Kay JN, et al. Retinal ganglion cells with distinct directional preferences differ in molecular identity, structure, and central projections. J. Neurosci. 2011; 31:7753–62. [PubMed: 21613488]

Kay JN, Chu MW, Sanes JR. MEGF10 and MEGF11 mediate homotypic interactions required for mosaic spacing of retinal neurons. Nature. 2012; 483:465–469. [PubMed: 22407321]

Keeley PW, et al. Dendritic spread and functional coverage of starburst amacrine cells. J. Comp. Neurol. 2007; 505:539–546. [PubMed: 17924572]

Keeley PW, Reese BE. Morphology of dopaminergic amacrine cells in the mouse retina: Independence from homotypic interactions. J. Comp. Neurol. 2010a; 518:1220–1231. [PubMed: 20148440]

Keeley PW, et al. Development and plasticity of outer retinal circuitry following genetic removal of horizontal cells. J. Neurosci. 2013; 33:17847–17862. [PubMed: 24198374]

Keeley PW, Reese BE. The patterning of retinal horizontal cells: normalizing the regularity index enhances the detection of genomic linkage. Front. Neuroanat. 2014; 8:113. [PubMed: 25374512]

Keeley PW, et al. Independent genomic control of neuronal number across retinal cell types. Develop. Cell. 2014a; 30:103–109.

Keeley PW, et al. Pituitary tumor transforming gene 1 regulates the patterning of retinal mosaics. Proc. Nat'l. Acad. Sci. U S A. 2014b; 111:9295–9300.

Keeley PW, et al. Programmed cell death of retinal cone bipolar cells is independent of afferent or target control. Dev. Biol. 2014c; 394:191–196. [PubMed: 25169191]

Keeley, PW.; Whitney, IE.; Reese, BE. Genomic control of retinal cell number: Challenges, protocol, and results. In: Schughart, K.; Williams, RW., editors. Molecular Methods in Biology: Genetics Systems. Springer; 2016. Vol., in press

Kim I-B, et al. Choline acetyltransferase-immunoreactive neurons in the developing rat retina. J. Comp. Neurol. 2000; 427:604–616. [PubMed: 11056467]

Kwasnieski JC, et al. Complex effects of nucleotide variants in a mammalian cis-regulatory element. Proc. Natl. Acad. Sci. U S A. 2012; 109:19498–19503. [PubMed: 23129659]

Lee SC, et al. Homotypic regulation of neuronal morphology and connectivity in the mouse retina. J. Neurosci. 2011; 31:14126–14133. [PubMed: 21976497]

Lin B, Wang SW, Masland RH. Retinal ganglion cell type, size, and spacing can be specified independent of homotypic dendritic contacts. Neuron. 2004; 43:475–485. [PubMed: 15312647]

Linden, R.; Reese, BE. Programmed cell death. In: Sernagor, E.; Eglen, S.; Harris, B.; Wong, R., editors. Retinal Development. Cambridge University Press; Cambridge: 2006. p. 208-241.Vol.

Macosko EZ, et al. Highly parallel genome-wide expression profiling of individual cells using nanoliter droplets. Cell. 2015; 161:1202–1214. [PubMed: 26000488]

Matsushima D, Heavner W, Pevny LH. Combinatorial regulation of optic cup progenitor cell fate by SOX2 and PAX6. Development. 2011; 138:443–454. [PubMed: 21205789]

Mojsin M, et al. Comparative analysis of SOX3 protein orthologs: Expansion of homopolymeric amino acid tracts during vertebrate evolution. Biochem. Genet. 2010; 48:612–623. [PubMed: 20495863]

Mu, X.; Klein, WH. Gene regulatory networks and retinal ganglion cell development. In: Chlupa, LM.; Williams, RW.; Eye Retina System Visual the of Mouse Vol. , editors. Massachusetts Institute of Technology; Cambridge: 2008. p. 321-332.

Ohsawa R, Kageyama R. Regulation of retinal cell fate specification by multiple transcription factors. Brain Res. 2008; 1192:90–98. [PubMed: 17488643]

Pei D. Regulation of pluripotency and reprogramming by transcription factors. J. Biol. Chem. 2009; 284:3365–3369. [PubMed: 18819918]

Poché RA, et al. Somal positioning and dendritic growth of horizontal cells are regulated by interactions with homotypic neighbors. Europ. J. Neurosci. 2008; 27:1607–1614.

Raven MA, Reese BE. Mosaic regularity of horizontal cells in the mouse retina is independent of cone photoreceptor innervation. Invest. Ophthalmol. Vis. Sci. 2003; 44:965–973. [PubMed: 12601016]

Raven MA, et al. Developmental improvement in the regularity and packing of mouse horizontal cells: Implications for mechanisms underlying mosaic pattern formation. Vis. Neurosci. 2005b; 22:569–573. [PubMed: 16332267]

Reese BE, Raven MA, Stagg SB. Afferents and homotypic neighbors regulate horizontal cell morphology, connectivity and retinal coverage. J. Neurosci. 2005; 25:2167–2175. [PubMed: 15745942]

Reese, BE. Mosaics, tiling and coverage by retinal neurons. In: Masland, RH.; Albright, T., editors. The Vision Senses: Comprehensive A Reference. Vol. 1. Elsevier, Oxford: 2008a. p. 439-456.Ch. 22

Reese BE, et al. Developmental plasticity of dendritic morphology and the establishment of coverage and connectivity in the outer retina. Dev. Neurobiol. 2011; 71:1273–1285. [PubMed: 21557509]

Reese BE, Keeley PW. Design principles and developmental mechanisms underlying retinal mosaics. Biol. Rev. 2015; 90:854–876. [PubMed: 25109780]

Reuveni E, Birney E, Gross CT. The consequence of natural selection on genetic variation in the mouse. Genomics. 2010; 95:196–202. [PubMed: 20171270]

Rivlin-Etzion M, et al. Transgenic mice reveal unexpected diversity of on-off direction-selective retinal ganglion cell subtypes and brain structures involved in motion processing. J. Neurosci. Meth. 2011; 31:8760–8769.

Rossi EA, Roorda A. The relationship between visual resolution and cone spacing in the human fovea. Nat. Neurosci. 2010; 13:156–157. [PubMed: 20023654]

Sanes JR, Masland RH. The types of retinal ganglion cells: current status and implications for neuronal classification. Ann. Rev. Neurosci. 2015; 38:221–246. [PubMed: 25897874]

Schneider A, et al. Novel SOX2 mutations and genotype-phenotype correlation in anophthalmia and microphthalmia. Am. J. Med. Genet. A. 2009; 149A:2706–2715. [PubMed: 19921648]

Singer JB, et al. Genetic dissection of complex traits with chromosome substitution strains of mice. Science. 2004; 304:445–448. [PubMed: 15031436]

Spalding KL, Rush RA, Harvey AR. Target-derived and locally derived neurotrophins support retinal ganglion cell survival in the neonatal rat retina. J. Neurobiol. 2004; 60:319–327. [PubMed: 15281070]

Spear PD, et al. Relationship between numbers of retinal ganglion cells and lateral geniculate neurons in the rhesus monkey. Vis. Neurosci. 1996; 13:199–203. [PubMed: 8731000]

Strettoi E, Volpini M. Retinal organization in the Bcl-2-overexpressing transgenic mouse. J. Comp. Neurol. 2002; 446:1–10. [PubMed: 11920715]

Swaroop A, Kim D, Forrest D. Transcriptional regulation of photoreceptor development and homeostasis in the mammalian retina. Nat. Rev. Neurosci. 2010; 11:563–576. [PubMed: 20648062]

Taranova OV, et al. SOX2 is a dose-dependent regulator of retinal neural progenitor competence. Genes Dev. 2006; 20:1187–1202. [PubMed: 16651659]

Thiel G, Lietz M, Hohl M. How mammalian transcriptional repressors work. Europ. J. Biochem. 2004; 271:2855–2862. [PubMed: 15233782]

Tong Y, Eigler T. Transcriptional targets for pituitary tumor-transforming gene-1. J. Mol. Endocrinol. 2009; 43:179–185. [PubMed: 19433493]

Vaney DI, Sivyer B, Taylor WR. Direction selectivity in the retina: symmetry and asymmetry in structure and function. Nat Rev Neurosci. 2012; 13:194–208. [PubMed: 22314444]

Voyatzis S, et al. Modeling activity and target-dependent developmental cell death of mouse retinal ganglion cells ex vivo. PLoS One. 2012; 7:e31105. [PubMed: 22363559]

Wang S, et al. A gene regulatory network controls the binary fate decision of rod and bipolar cells in the vertebrate retina. Dev. Cell. 2014; 30:513–527. [PubMed: 25155555]

Wässle H, Riemann HJ. The mosaic of nerve cells in the mammalian retina. Proc. R. Soc. Lond B. 1978; 200:441–461. [PubMed: 26058] Wässle H, et al. Cone contacts, mosaics and territories of bipolar cells in the mouse retina. J. Neurosci. 2009; 29:106–117. [PubMed: 19129389]

Whitney IE, et al. Spatial patterning of cholinergic amacrine cells in the mouse retina. J. Comp. Neurol. 2008; 508:1–12. [PubMed: 18288692]

Whitney IE, et al. Multiple genes on chromosome 7 regulate dopaminergic amacrine cell number in the mouse retina. Invest. Ophthalmol. Vis. Sci. 2009; 50:1996–2003. [PubMed: 19168892]

Whitney IE, et al. A QTL on chromosome 10 modulates cone photoreceptor number in the mouse retina. Invest. Ophthalmol. Vis. Sci. 2011a; 52:3228–3236. [PubMed: 21330668]

Whitney IE, et al. Genetic modulation of horizontal cell number in the mouse retina. Proc. Nat'l. Acad. Sci. U S A. 2011b; 108:9697–9702. [PubMed: 21576457]

Whitney IE, et al. Sox2 regulates cholinergic amacrine cell positioning and dendritic stratification in the retina. J. Neurosci. 2014; 34:10109–10121. [PubMed: 25057212]

Williams RW, et al. Genetic and environmental control of variation in retinal ganglion cell number in mice. J. Neurosci. 1996; 16:7193–7205. [PubMed: 8929428]

Williams RW, et al. The genetic structure of recombinant inbred mice: high-resolution consensus maps for complex trait analysis. Gen. Biol. 2001; 2 research0046.1-0046.18.

Xiang M. Intrinsic control of mammalian retinogenesis. Cell. Mol. Life Sci. 2013; 70:2519–2532. [PubMed: 23064704]

Xin D, Bloomfield SA. Dark- and light-induced changes in coupling between horizontal cells in mammalian retina. J. Comp. Neurol. 1999; 405:75–87. [PubMed: 10022197]

Young RW. Cell differentiation in the retina of the mouse. Anat. Rec. 1985; 212:199–205. [PubMed: 3842042]

Zhang TJ, et al. Variability in human cone topography assessed by adaptive optics scanning laser ophthalmoscopy. Am. J Ophthalmol. 2015; 160:290–300. [PubMed: 25935100]

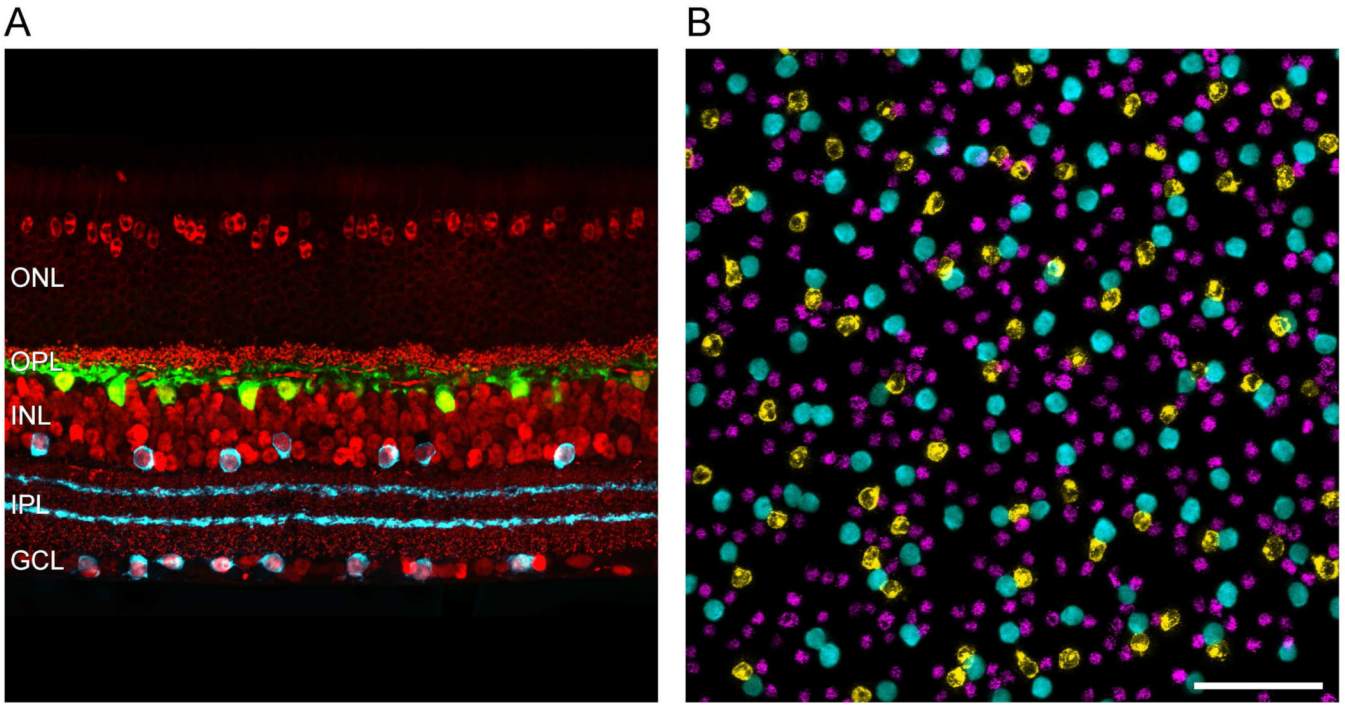

Figure 1.

The retinal architecture is composed of five major classes of retinal neurons, being the photoreceptor cells, horizontal cells, bipolar cells, amacrine cells and ganglion cells. Each class is composed of multiple types which, together, approach perhaps as many as 85 different cell types in the mouse retina (Sanes and Masland, 2015). The developmental program generates a particular number of each cell type, which can vary by four orders of magnitude across these different cell types. A: Those different cell types become positioned in at specific depths within the retina, shown here for the cone photoreceptors in the outer nuclear layer at the top (in red, labeled for CtBP2), the horizontal cells (in green, labeled for calbindin), and the cholinergic amacrine cells (in cyan, labeled for choline acetyltransferase). B: Within each population, the cells are typically distributed as regular arrays of cells, commonly referred to as “retinal mosaics”, shown here for the VGluT3 amacrine cells (in yellow, labeled for the vesicular glutamate transporter 3), the AII amacrine cells (in magenta, labeled for Prox1), and the cholinergic amacrine cells in the inner nuclear layer (in cyan), ensuring a uniformity in their contribution to retinal processing across the visual scene. Calibration bar = 50 μm.

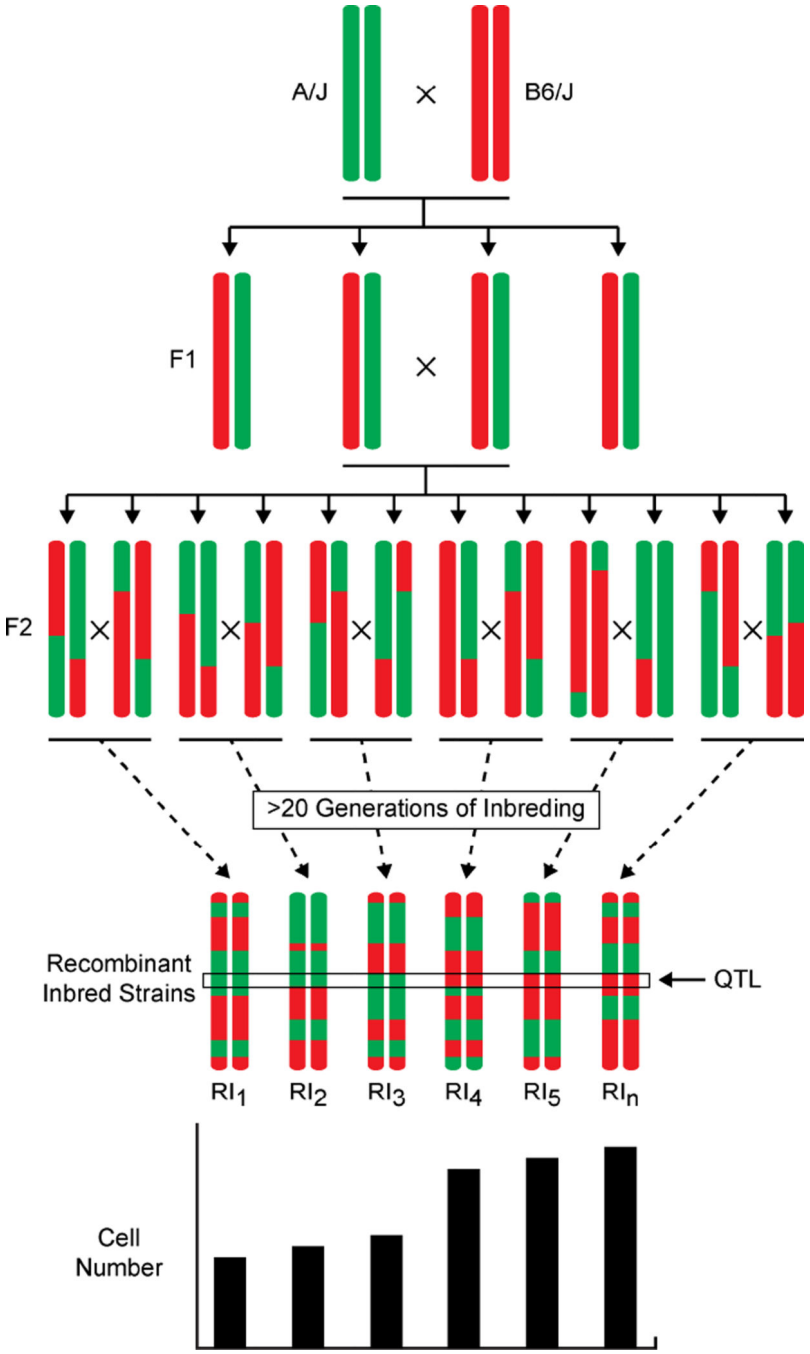

Figure 2.

Recombinant inbred strains of mice provide a resource for locating regions in the genome that contribute to the variation in any quantifiable trait of interest. Recombinant inbred strains are generated by inbreeding different pairs of F2 offspring following an initial cross of the two parental strains (in this case, the B6/J and A/J inbred strains), to yield mice that are homozygous for either the *B* or the *A* haplotype throughout the genome. Each recombinant inbred strain differs in the unique assembly of the two haplotypes due to random recombination events during meiosis. This variation in the presence of the two

haplotypes (known through genotyping each strain with high density SNPs and microsatellite markers that discriminate the two parental genomes) can be compared with the variation in cell number, permitting an assessment of the strength of linkage between genotype and phenotype across the genome. Where linkage is strong at a particular genomic locus, it is termed a quantitative trait locus (QTL), where genetic variants must contribute to the variation in cell number.

A

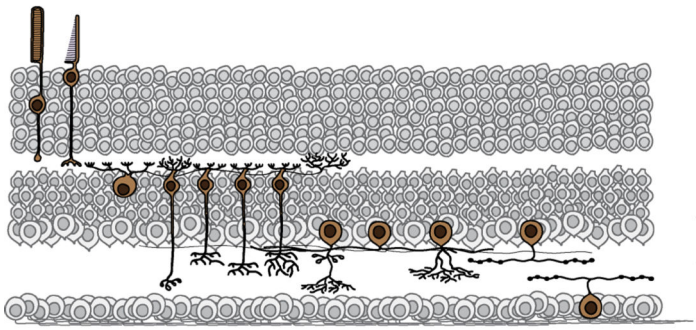

C

Cell Type	Range	% Increase	CoV
Rod Photoreceptors	6,051,100 - 8,227,260	36	0.036
Cone Photoreceptors	116,158 - 204,419	76	0.061
Horizontal Cells	9,884 - 18,942	92	0.034
Rod Bipolar Cells	202,415 - 254,176	26	0.046
Type 2 Cone Bipolar Cells	41,908 - 60,570	45	0.046
Type 3b Cone Bipolar Cells	50,243 - 80,469	60	0.050
Type 4 Cone Bipolar Cells	29,351 - 50,260	71	0.065
AII Amacrine Cells	57,141 - 86,557	51	0.046
Dopaminergic Amacrine Cells	160 - 637	298	0.045
VGluT3+ Amacrine Cells	10,415 - 14,857	43	0.030
Cholinergic Amacrine Cells (INL)	14,505 - 22,304	54	0.041
Cholinergic Amacrine Cells (GCL)	12,434 - 18,414	48	0.040

B

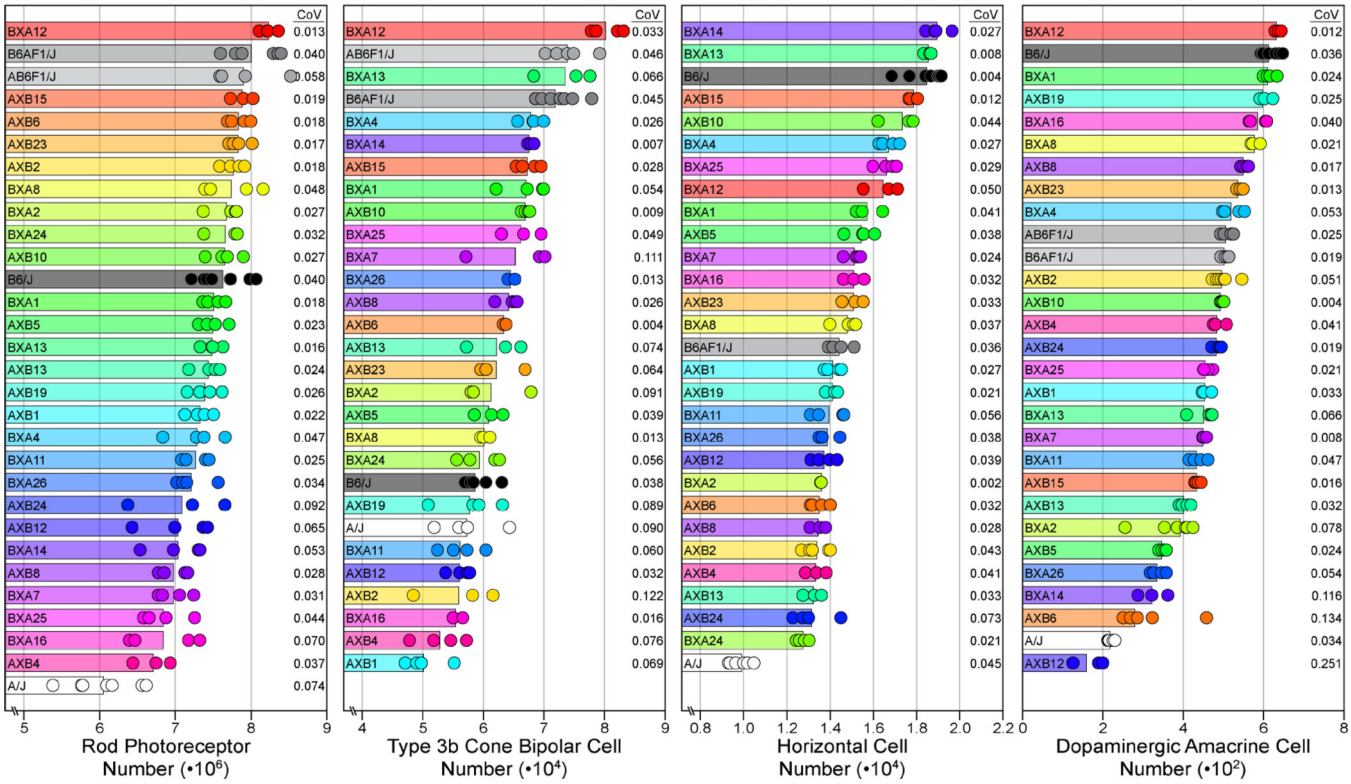

Figure 3.

The total numbers of twelve different retinal cell types were determined in the 26 recombinant inbred strains of the AXB/BXA strain-set. A: Schematic indicating the particular types of neurons quantified, including (from left to right) rod and cone photoreceptors, horizontal cells, rod bipolar cells, Types 2, 3b and 4 cone bipolar cells, and AII amacrine cells, dopaminergic amacrine cells, VGluT3+ amacrine cells, and cholinergic amacrine cells positioned in either the INL or GCL. B: The numbers of four of these different types in each of the mice (colored circles) analyzed from this strain-set. Those mice of the same recombinant inbred strain share the same color, while the parental strains are indicated in black (B6/J) and white (A/J), and the F1 strains are indicated in grey. The bars of the histogram, for each cell type, indicate the strain means and standard errors,

descending from highest to the lowest. The coefficient of variation for each strain (CoV; the ratio of the standard deviation to the mean) is indicated to the right of each bar. Notice that the ordinal position of a strain can vary conspicuously across the different cell types. For instance, the AXB6 strain, in orange, is shifted progressively to lower relative numbers across the four cell types illustrated. C: The range of variation across the strains, from lowest to highest strain average, for each cell type is indicated, expressed also as the percent increase from lowest to highest strain, along with the average CoV across all of the strains, for each cell type. (Modified from Keeley et al., 2014a.)

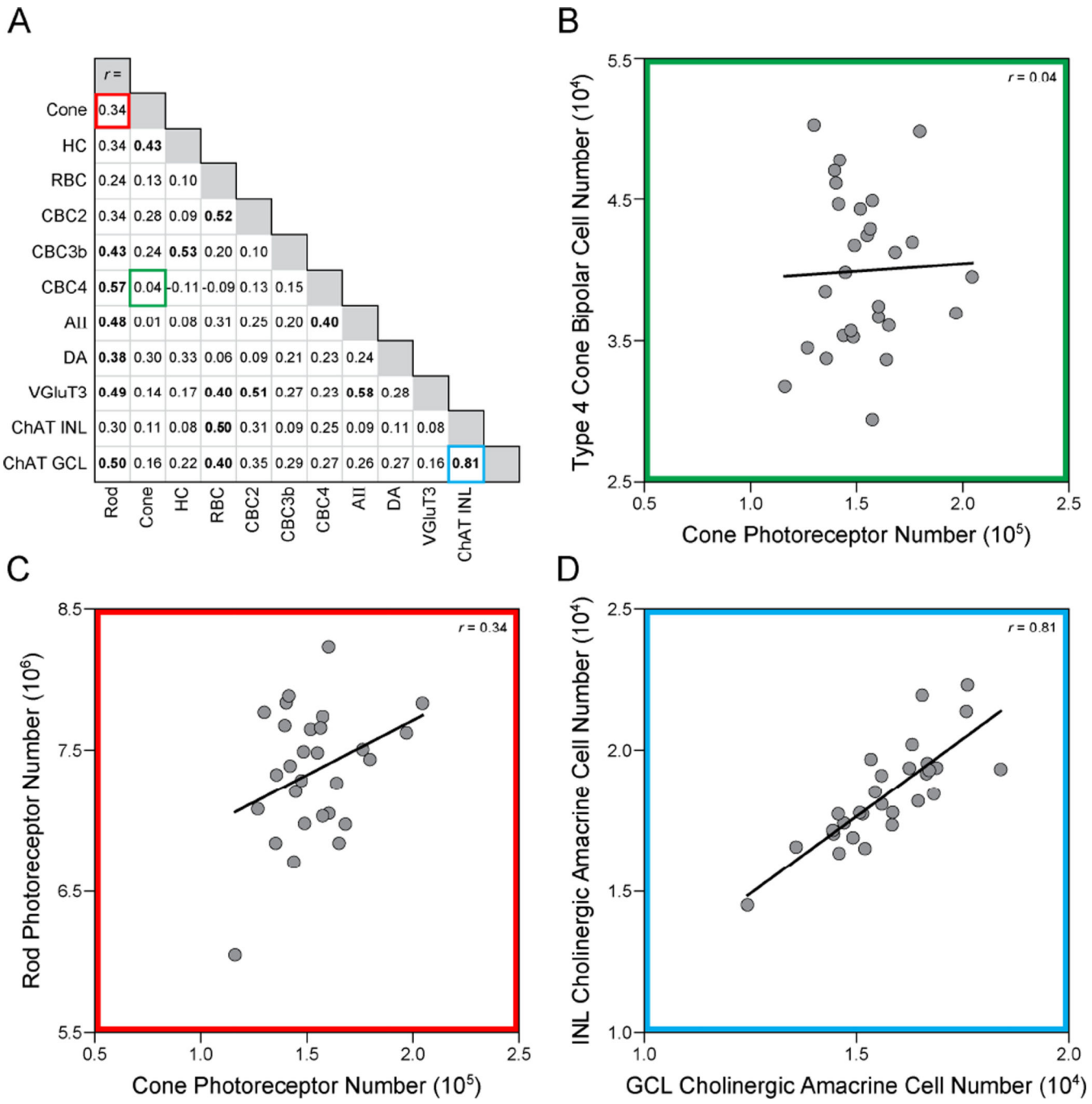

Figure 4.

Pearson correlation coefficients (*r*) were calculated for every pair-wise comparison of the strain averages across the twelve different cell types. A: The correlation matrix indicates the *r* for each linear regression, with significant correlation coefficients (p value < 0.05) being emboldened. B-D: Scatterplots showing the data for three different comparisons: for Type 4 cone bipolar cells and cone photoreceptors (B), for rod and cone photoreceptors (C), and for the two populations of cholinergic amacrine cells in the INL and GCL (D). For most comparisons, particularly those between cell types that share transcriptional control (e.g. the

rod and cone photoreceptors) or those that define the radial transmission of visual information through the retina (e.g. the cones and cone bipolar cells), there is no significant relationship. Cholinergic amacrine cells in the two layers are the exception, showing a strong correlation in their numbers across the strains. (Modified from Keeley et al., 2014a and Whitney et al., 2014).

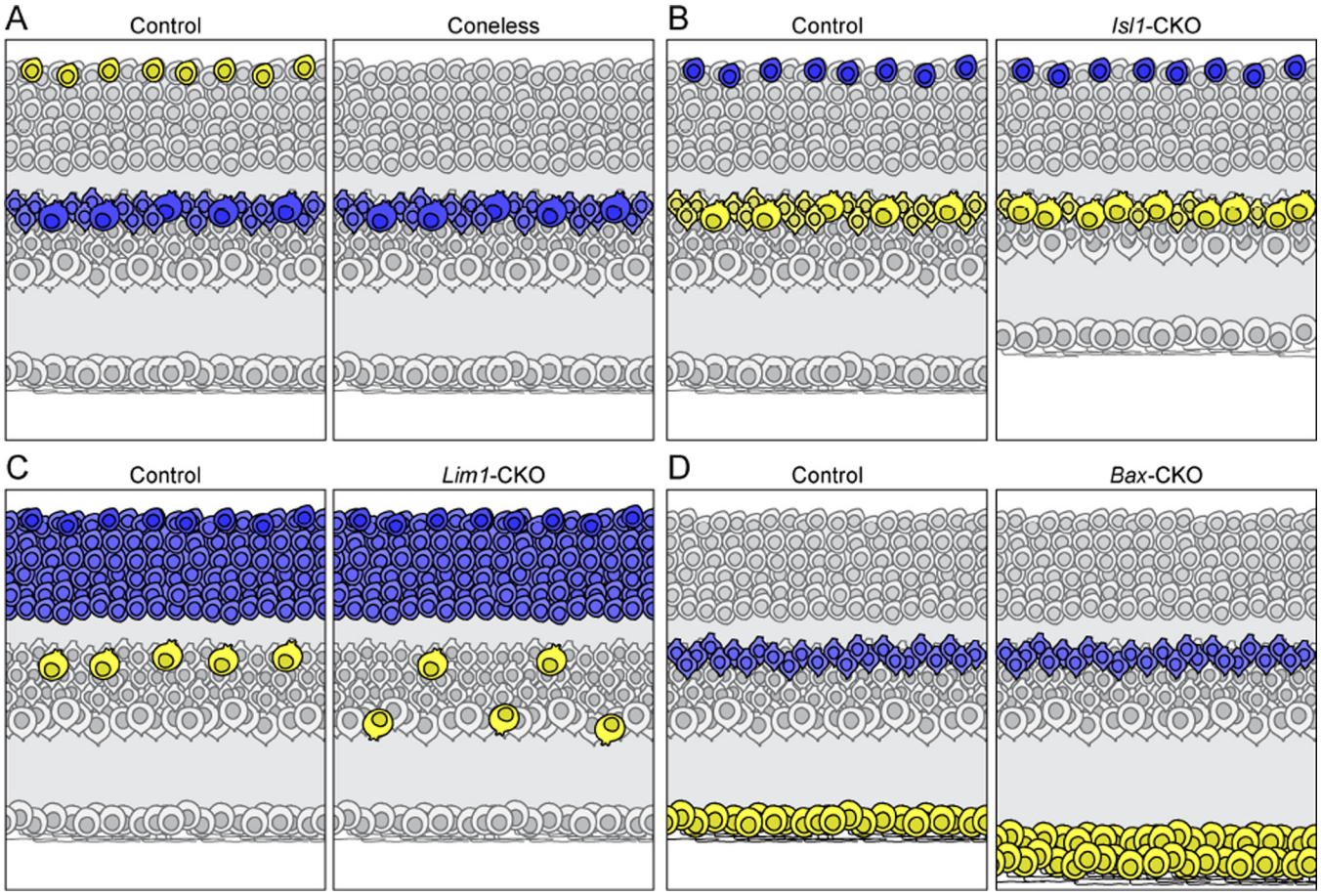

Figure 5.

Genetic manipulations that alter the number of targets or afferents in the retina do not modulate neuronal number. A: Coneless mutant mice lose nearly all of their cones during the first postnatal week (yellow), yet the numbers of target neurons in the inner nuclear layer in maturity is unaffected (blue). B: *Isl1*-conditional knockout mice, that show a reduced number of bipolar cells and an increased number of horizontal cells (yellow), leave the number of cone photoreceptors unaffected (blue). C: *Lim1*-conditional knockout mice, that reduce the number of horizontal cells contributing processes to the outer plexiform layer (yellow), do not alter the numbers of cone or rod photoreceptors (blue). D: Retinal ganglion cell-specific *Bax*-conditional knockout mice, having excess retinal ganglion cells (yellow), do not support a larger than normal number of cone bipolar cells (blue).

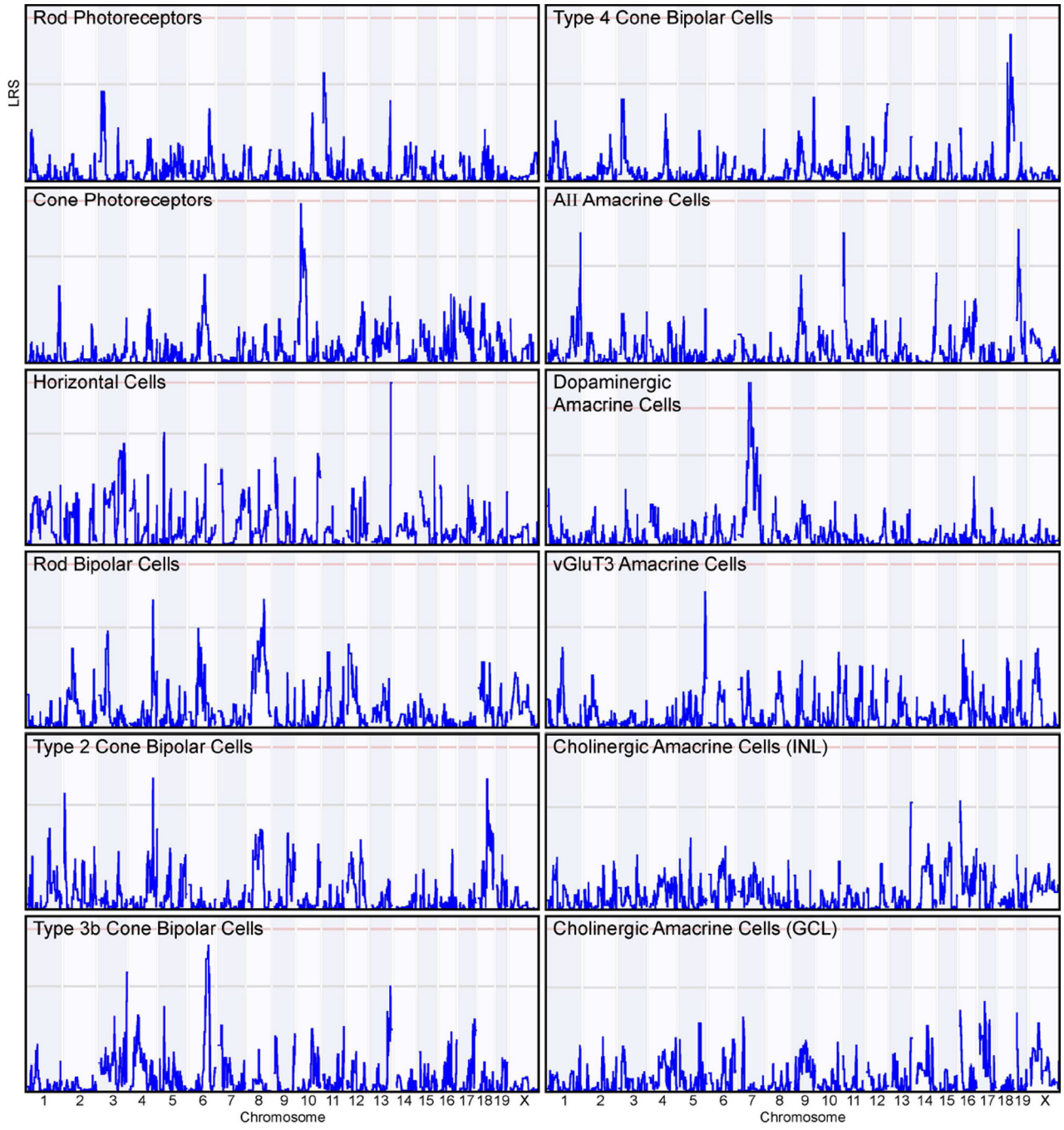

Figure 6.

The variation in the numbers of each type of retinal neuron map to genomic loci (QTL) that are largely independent of one another. Each genomic map shows strength of linkage between genotype (being the *A* versus *B* haplotype) and phenotype (the number of a particular cell type). The trace shows the likelihood ratio statistic (LRS), assessing the strength of this linkage between cell number and genomic locus, across the genome, while the horizontal lines define significant and suggestive thresholds determined through

permutation testing of the strain data. Genetic variants that discriminate the parental genomes at these largest peak loci should contribute to the variation in phenotype.

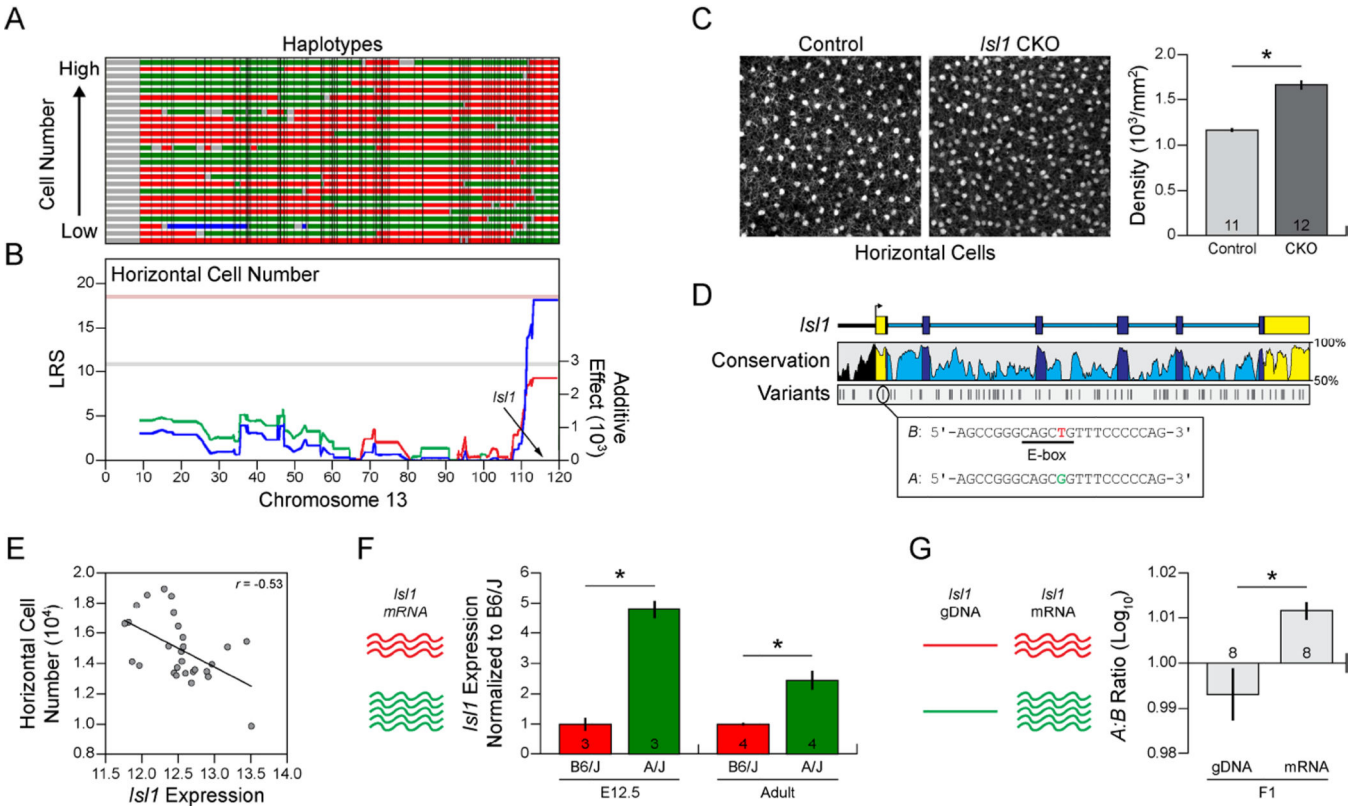

Figure 7.

Variation in the number of horizontal cells maps to a distal locus on Chr 13. A: The variation in haplotype on Chr 13 across the strains, here ranked by the variation in horizontal cell number across the strains (shown in figure 3B), reveals the basis for identifying the QTL at the distal locus on Chr 13 (shown in figure 6). B: The map of Chr 13 is aligned directly beneath the haplotypes, showing the effect of the *B* haplotype at this locus, indicated by the red trace, contributing an additive effect of 2490 cells. The magnitude of this QTL effect is 28% of the range observed across the recombinant inbred strains. The transcription factor gene *Isl1* is positioned at this locus. C: The density of horizontal cells is significantly increased in the *Isl1*-conditional knockout mouse retina. D: No functional variants discriminate the parental genomes, but numerous potential regulatory variants are present, including one in a genomic region that is highly conserved across species (shown is the percent of conservation between mouse and human genomes). The T for G substitution is the novel variant, establishing a hexanucleotide “E-box” sequence in the 5´UTR in the B6/J genome. E: Horizontal cell number is negatively correlated with *Isl1* expression across the recombinant inbred strains. F: qPCR confirms significantly greater expression in the A/J strain in maturity as well as during embryonic development, when horizontal cells are being generated. G: *Isl1 A* allele transcripts significantly outnumber *Isl1 B* allele transcripts in the F1 progeny of a cross between the parental strains, confirming that at least a portion of the expression difference between the parental strains must be *cis*-regulated.

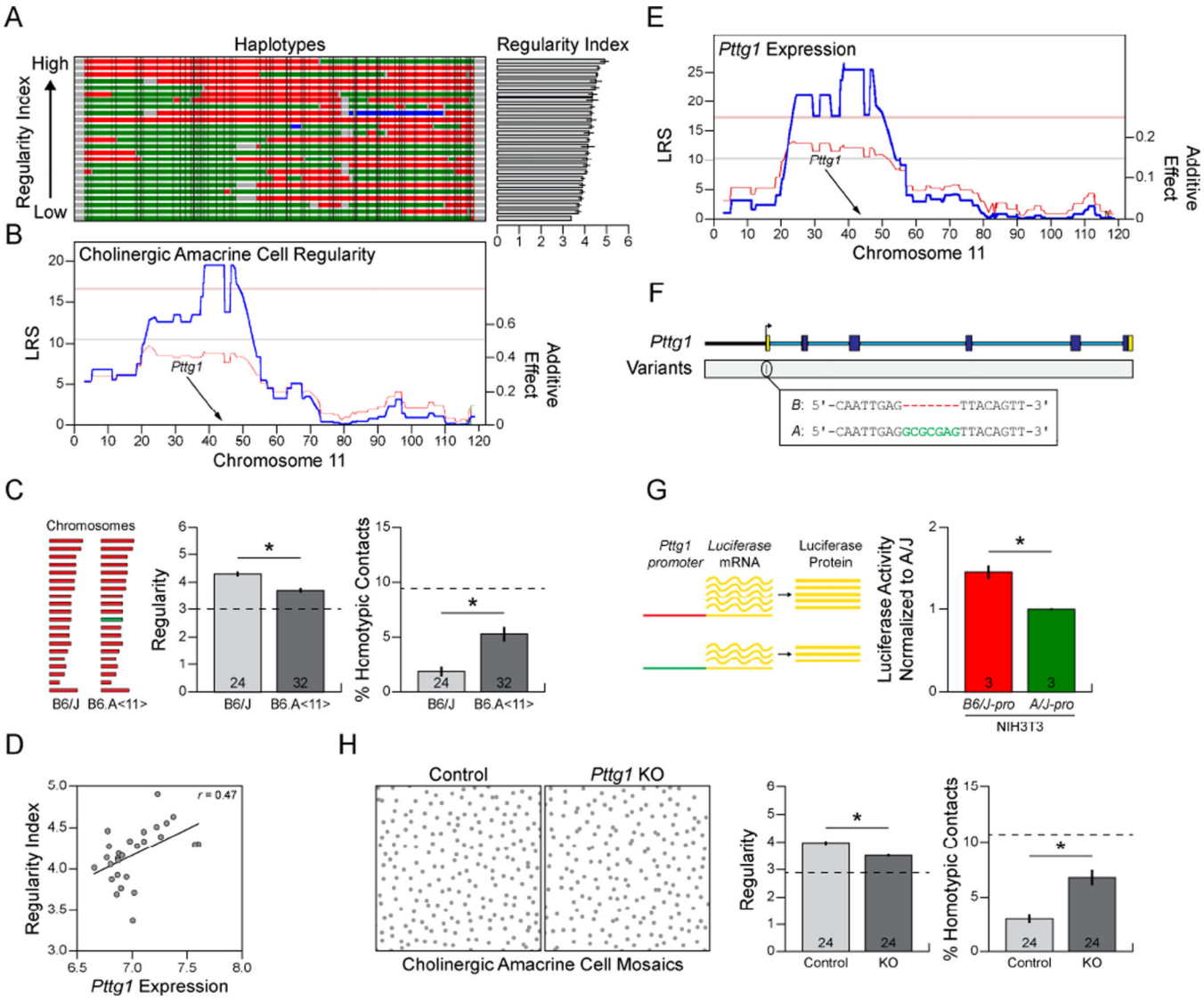

Figure 8.

Genes controlling other demographic traits associated with retinal cell populations can be identified using this same forward-genetic approach. A: The regularity index, derived from the distribution of nearest neighbor distances for the population of cholinergic amacrine cells in the inner nuclear layer, shows conspicuous variation across the strains, correlating with the variation in haplotype to a locus on Chr 11. B: The variation maps a significant QTL, where the presence of the B haplotype is associated with an increase in regularity. C: The chromosome substitution strain B6.A<11>, containing the *A* haplotype throughout Chr 11 on a C57BL/6J genetic background, confirms the presence of genetic variants on Chr 11 affecting mosaic regularity. B6.A<11> mice show a significant reduction in regularity and a significant increase in the number of cells that fail to space themselves apart. D: The regularity index correlates with the expression of *Pttg1* across the recombinant inbred strains. E: Expression of *Pttg1* maps an expression QTL (eQTL) to the same genomic locus, suggesting the presence of a *cis*-regulatory variant. F: A seven-nucleotide deletion at the

transcriptional start-site discriminates the B6/J strain from the A/J strain (inset), being the only variant present. G: Luciferase assay showed the *B* variant to be a significantly more effective transcriptional activator than the *A* variant. H: *Ptg1* knockout mice show a significant reduction in mosaic regularity and a significant increase in the frequency of neighboring cells that fail to space themselves apart. Dashed horizontal lines in C and H indicate the values associated with random distributions matched in density and constrained by soma size (Modified from Keeley et al., 2014b).

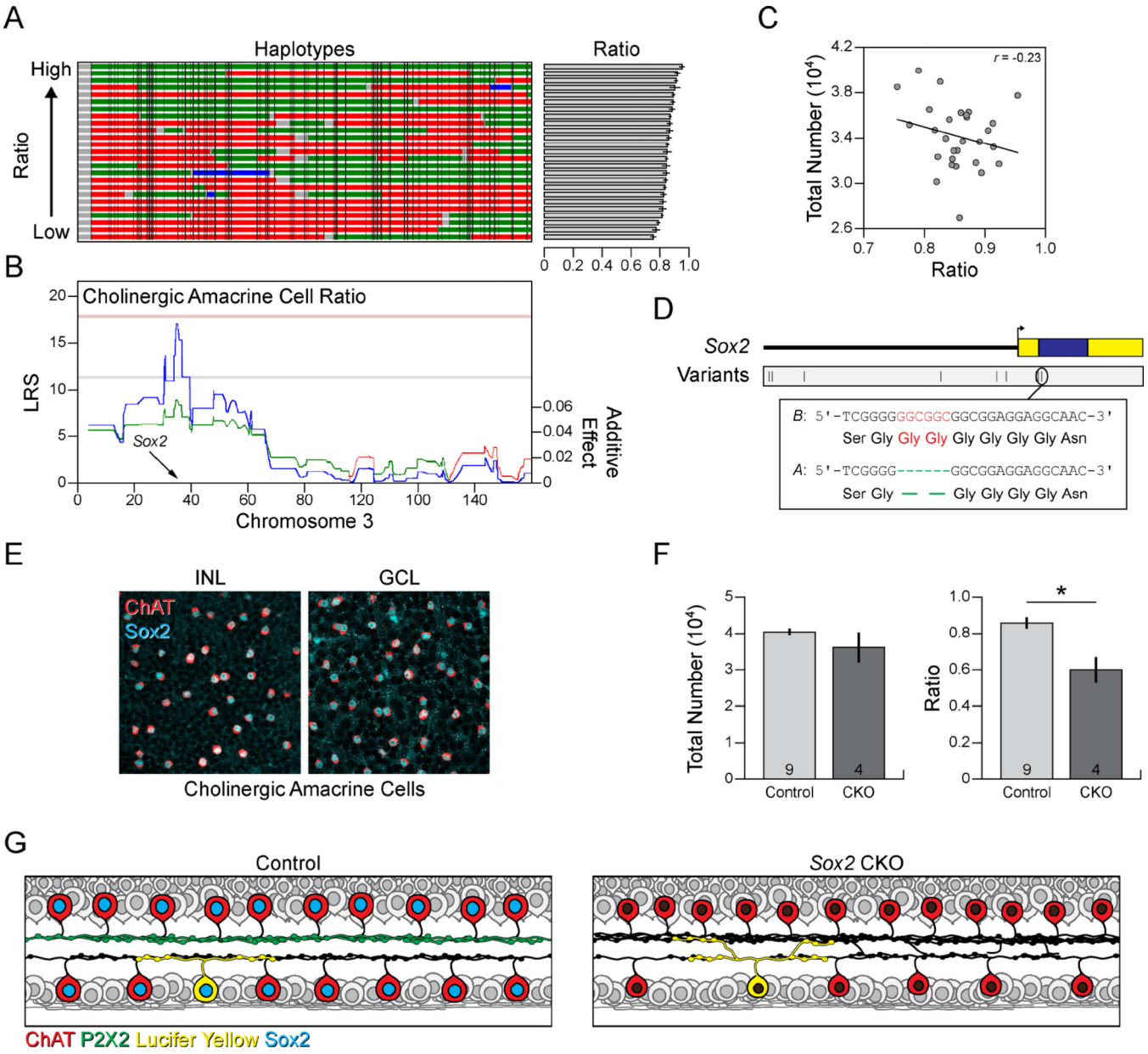

Figure 9.

Sox2 is a candidate gene modulating the positioning of cholinergic amacrine cells in the GCL versus the INL. A: Cholinergic amacrine cells are positioned in both the INL and GCL, always being slightly more numerous in the INL. This ratio of cells in the two layers (GCL/INL) is also a heritable trait. B: The variation in this ratio trait maps a QTL on Chr 3, where the *A* haplotype correlates with an increase in this ratio, driving it towards parity. C: This ratio trait shows no correlation with the total number of cholinergic amacrine cells, indicating a difference in the relative positioning of the two cell types rather than being due to the modulation of the size of one of their two populations (p = 0.2). D: A six-nucleotide insertion in the B6/J strain extends a polyglycine tract in Sox2. E: The candidate gene, *Sox2*, is expressed exclusively by cholinergic amacrine cells amongst neuronal populations in the

mature retina. F: *Sox2* conditional knockout mice show a mis-positioning of their cholinergic amacrine cells between the two layers, though show no significant difference in their total numbers. G: The loss of *Sox2* modulates sub-type specification, rather than simply migration, as other discriminating features of the ON from OFF cholinergic amacrine cells are altered, for instance, the entire loss of P2×2 labeling, and the novel presence of bistratifying dendrites (Modified from Whitney et al., 2014.)

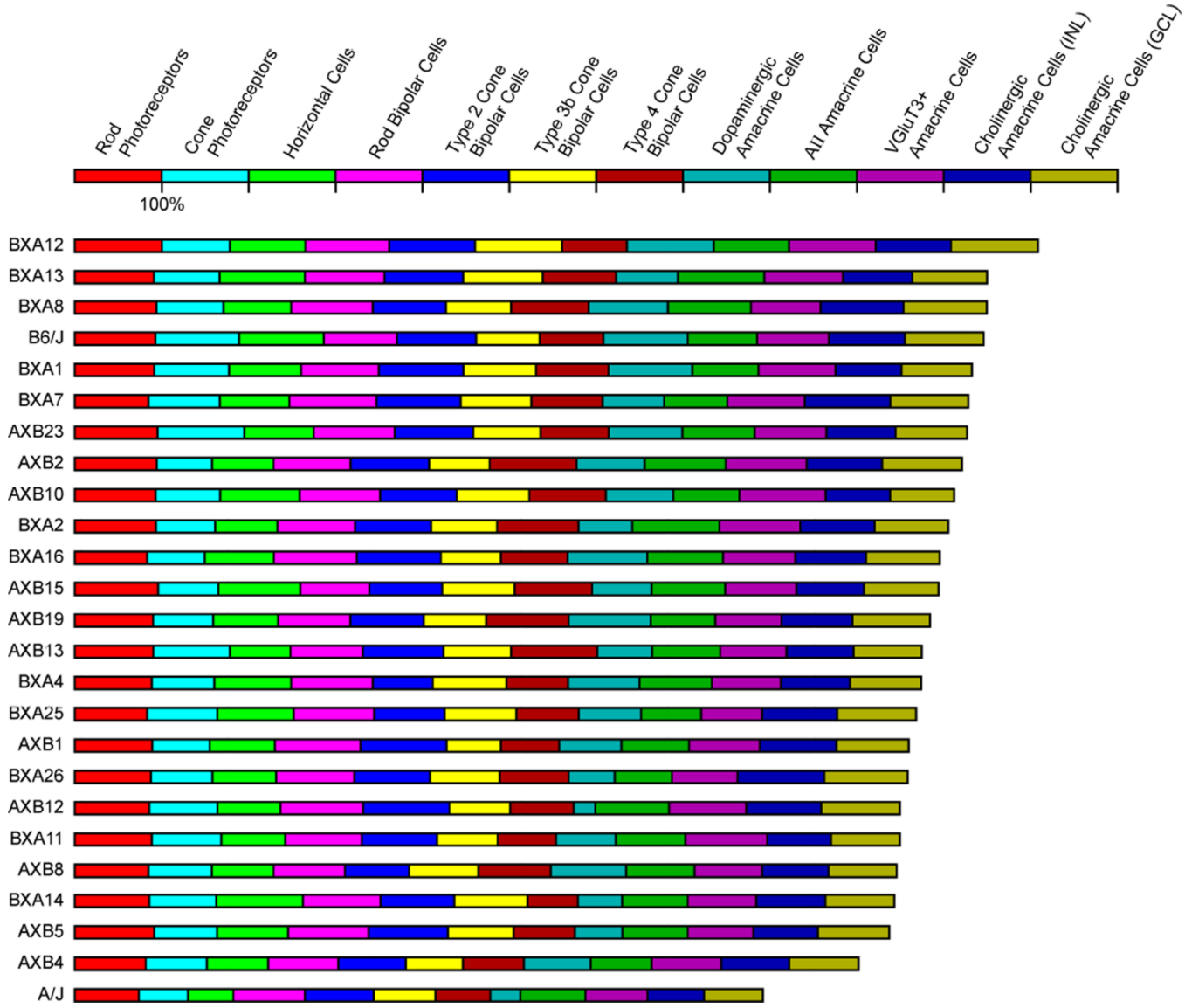

Figure 10.

Each strain contains its own unique mix of the twelve different retinal cell populations identified. The magnitude of the different cellular populations is ignored here; rather, each population has been normalized to the maximal number observed (i.e. in the strain with the greatest number), to portray the variation in each strain across all of the cell types relative to that maximum number. (Only those strains for which every cell type had been sampled are included herein—see Table S1 in Keeley et al., 2014a).